An environmentally-benign CeO$_2$-TiO$_2$ catalyst for the selective catalytic reduction of NO$_x$ with NH$_3$ in simulated diesel exhaust

Wenpo Shan [a,b], Fudong Liu [a,*], Hong He [a,*], Xiaoyan Shi [a], Changbin Zhang [a]

[a] Research Center for Eco-Environmental Sciences, Chinese Academy of Sciences, Beijing 100085, PR China
[b] College of Chemistry and Environmental Science, Hebei University, Baoding 071002, PR China

ARTICLE INFO

ABSTRACT

A Ce-Ti based (CeO$_2$-TiO$_2$) catalyst prepared by an optimized homogeneous precipitation method showed excellent NH$_3$-SCR activity, high N$_2$ selectivity, broad operation temperature window, and high resistance to space velocity (even under a high gas hourly space velocity (GHSV) of 500,000 h^{-1}). Compared with V$_2$O$_5$-WO$_3$/TiO$_2$ and Fe-ZSM-5 catalysts, the CeO$_2$-TiO$_2$ catalyst showed better catalytic performance for NH$_3$-SCR. Under a more realistic condition of simulated diesel engine exhaust, the monolith catalyst of CeO$_2$-TiO$_2$ showed over 90% NO$_x$ conversion from 250 to 450 °C under a GHSV of 20,000 h^{-1} in the presence of H$_2$O, CO$_2$, and C$_3$H$_6$. The high dispersion of active CeO$_2$ on TiO$_2$ in the process of homogenous precipitation and the synergistic effects between CeO$_2$ and TiO$_2$ in CeO$_2$-TiO$_2$ are important reasons for the high NH$_3$-SCR activity.

© 2011 Elsevier B.V. All rights reserved.

1. Introduction

Compared with gasoline engines, highly fuel efficient diesel engines could reduce fuel consumption and decrease the production of greenhouse gas carbon dioxide (CO$_2$). However, the emission of NO$_x$ remains a major constraint of diesel engines [1–3]. Selective catalytic reduction of NO$_x$ by NH$_3$ (NH$_3$-SCR) is one of the most promising NO$_x$ control strategies for lean burn engines, particularly diesel engines, to meet the increasingly stringent standards for NO$_x$ emissions [1]. The high NO$_x$ removal efficiency by NH$_3$-SCR allows fuel sensitive applications to be run at maximum efficiency (high NO$_x$, low PM), which could offer significant fuel savings (about 8% with respect to exhaust gas recirculation (EGR) systems) [2].

NH$_3$-SCR over V$_2$O$_5$-WO$_3$(or MoO$_3$)/TiO$_2$ has been widely used for many decades and is still the best commercial technology for NO$_x$ abatement from stationary sources [4,5]. Vanadium-based catalysts were also introduced into the diesel vehicle market due to their effectiveness for NH$_3$-SCR reaction and resistance to SO$_2$ poisoning [1,5]. However, the toxicity of active vanadium species, together with the large N$_2$O formation at high temperatures, has restrained its wider application, and vanadium-based SCR catalysts

for NO$_x$ removal from mobile sources will be gradually removed from the market over the next few years [2]. Therefore, great efforts have been made to develop environmentally-benign NH$_3$-SCR catalysts, with high SCR activity and N$_2$ selectivity in a wide temperature range, for controlling the NO$_x$ emissions from mobile sources such as diesel engines.

There are limitations to the catalyst volume that can be placed on board, which requires that the SCR catalyst should present superior NH$_3$-SCR performance under high space velocity conditions. Therefore, transition metal-exchanged zeolites, with high resistance to space velocity, have received increasing attention in recent years for the purpose of mobile application [6]. Particularly, iron or copper-exchanged zeolites have been extensively studied for their high catalytic activity and selectivity for N$_2$ production [7–11]. However, the insufficient low-temperature activity of iron-exchanged zeolites and the lack of hydrothermal stability of copper-exchanged zeolites have limited their industrial application [1,6,12]. Recently, some Cu-containing small-pore zeolites, such as Cu-SSZ-13 [13–15] and Cu-SAPO-34 [14], with remarkably improved hydrothermal stability, have been reported as promising candidates for the potential application in diesel engine exhaust treatment.

Some vanadium-free transition metal-based oxide catalysts, such as FeTiO$_x$ [16–18], CuO$_x$/WO$_x$-ZrO$_2$ [19], and WO$_3$/CeO$_2$-ZrO$_2$ [20], have also been reported as potential substitutes of vanadium-based catalysts for diesel vehicles. Nevertheless, these catalysts have been mainly tested under relatively low GHSV (<100,000 h^{-1}).

* Corresponding authors at: P.O. Box 2871, 18 Shuangqing Road, Haidian District, Beijing 100085, PR China. Tel.: +86 10 62911040/62849123; fax: +86 10 62911040/62849123.
E-mail addresses: fdliu@rcees.ac.cn (F. Liu), honghe@rcees.ac.cn (H. He).

Since the reduction of NH$_3$-SCR catalyst volume is one of the main challenges to diesel vehicles with limited space on board, it is very important to develop metal oxide catalysts with high resistance to space velocity [1,2].

Cerium has two stable oxidation states (Ce^{3+} and Ce^{4+}), which provide it with significant oxygen storage capability through the redox shift between the two oxidation states. Cerium has often been used as an additive to enhance the activity of various catalysts. For example, the addition of cerium enhances the NH$_3$-SCR activity and stability of Fe-ZSM-5 [7], V$_2$O$_5$-WO$_3$/TiO$_2$ [21], and MnO$_x$/TiO$_2$ [22]. In addition, some CeO$_2$-based catalysts, such as CeO$_2$-zeolite [23] and sulfated CeO$_2$ [24], are very active for NH$_3$-SCR reaction. In our previous study, we successfully developed a highly effective Ce/TiO$_2$ catalyst prepared by impregnation method for NH$_3$-SCR reaction [25]. We also recently improved the catalytic activity of a Ce-Ti based catalyst. The improved catalyst, prepared by a facile homogeneous precipitation method, showed relatively good SCR activity under a high GHSV of 150,000 h^{-1} due to the highly dispersed CeO$_2$ on TiO$_2$ [26]. In the present study, a Ce-Ti based catalyst (CeO$_2$-TiO$_2$) was prepared by an optimized homogeneous precipitation method. The CeO$_2$-TiO$_2$ catalyst exhibited an excellent performance under a GHSV of 250,000 h^{-1} in simulated diesel exhaust and even showed good resistance to a high GHSV of 500,000 h^{-1}, thus it is a potential candidate for practical application in the deNO$_x$ process for diesel engines.

2. Experimental

2.1. Catalyst synthesis and activity test

The CeO$_2$-TiO$_2$ catalyst was prepared by an optimized homogeneous precipitation method. The aqueous solutions of Ce(NO$_3$)$_3$·6H$_2$O and Ti(SO$_4$)$_2$ were mixed with a required molar ratio (Ce/Ti = 1:5). Excessive urea aqueous solution was then added into the mixed solution, with a urea/(Ce + Ti) molar ratio of 10:1. The mixed solution was then heated to 90 °C and held there for 12 h (to investigate the formation process of the CeO$_2$-TiO$_2$ catalyst, some samples with different precipitation time were also prepared) with vigorous stirring. After filtration and washing with deionized water, the resulting precipitant was dried at 100 °C overnight and subsequently calcined at 500 °C for 5 h in air conditions. Pristine CeO$_2$ and TiO$_2$ were also prepared using the same method as reference samples for activity tests and characterizations.

Before the NH$_3$-SCR activity test, the powder catalysts were pressed, crushed, and sieved to 40–60 mesh. To evaluate the CeO$_2$-TiO$_2$ catalyst under more practical conditions, a cylindrical cordierite honeycomb (300 cpsi) was washcoated by catalyst slurry. After drying at 100 °C overnight and subsequent calcination at 500 °C for 3 h in air conditions, the CeO$_2$-TiO$_2$ monolith catalyst with 130 g/L loading was obtained.

To comprehensively evaluate the activity of the CeO$_2$-TiO$_2$ catalyst in this study, conventional V$_2$O$_5$-WO$_3$/TiO$_2$ and Fe-ZSM-5 catalysts were prepared as reference materials. The V$_2$O$_5$-WO$_3$/TiO$_2$ catalyst with 4.5 wt.% V$_2$O$_5$ and 10 wt.% WO$_3$ was prepared by conventional impregnation method using NH$_4$VO$_3$, (NH$_4$)$_{10}$W$_{12}$O$_{41}$, and H$_2$C$_2$O$_4$·2H$_2$O as precursors and anatase TiO$_2$ as the support. After impregnation, the excess water was removed in a rotary evaporator at 80 °C. The sample was dried at 100 °C overnight and then calcined at 550 °C for 3 h in air conditions. The Fe-ZSM-5 catalyst with an iron loading of 7 wt.% was prepared by incipient wetness impregnation method using FeCl$_2$·4H$_2$O as the precursor and H-ZSM-5 (Si/Al = 25) as the support. We firstly dissolved FeCl$_2$·4H$_2$O in deionized water and then added H-ZSM-5 to form a paste. The paste was aged for 24 h at room temperature

and dried at 60 °C overnight. Finally, the sample was calcined in air conditions at 550 °C for 6 h.

The CeO$_2$-TiO$_2$ and V$_2$O$_5$-WO$_3$/TiO$_2$ catalysts calcined at 800 °C for 1 h in air conditions were also prepared to investigate their thermal stabilities for practical use, and were denoted as CeO$_2$-TiO$_2$-800 and V$_2$O$_5$-WO$_3$/TiO$_2$-800, respectively.

The SCR activity measurements were carried out in a fixed-bed quartz flow reactor at atmospheric pressure. The reaction conditions were controlled as follows: 500 ppm NO, 500 ppm NH$_3$, 5 vol.% O$_2$, [H$_2$O] = 5 vol.% (when used), [CO$_2$] = 5 vol.% (when used), [C$_3$H$_6$] = 500 ppm (when used), balance N$_2$, and 500 ml/min total flow rate. Different GHSVs were obtained by changing the volume of the catalyst. The effluent gas, including NO, NH$_3$, NO$_2$, and N$_2$O was continuously analyzed by an online NEXUS 670-FTIR spectrometer equipped with a gas cell with 0.2 dm^3 volume. The FTIR spectra were collected after 1 h when the SCR reaction reached a steady state. The NO$_x$ conversion and N$_2$ selectivity were calculated as follows [18,26,27]:

$$NO_x \text{ conversion} = \left(1 - \frac{[NO]_{out} + [NO_2]_{out}}{[NO]_{in} + [NO_2]_{in}}\right) \times 100\% \qquad (1)$$

$$N_2 \text{ selectivity} = \frac{[NO]_{in} + [NH_3]_{in} - [NO_2]_{out} - 2[N_2O]_{out}}{[NO]_{in} + [NH_3]_{in}} \times 100\%$$
$$(2)$$

2.2. Characterizations

The surface areas of the samples were obtained by N$_2$ adsorption/desorption analysis at −196 °C using a Quantachrome Quadrasorb SI-MP. Prior to the N$_2$ physisorption, the catalysts were degassed at 300 °C for 4 h. Surface areas were determined by BET equation in 0.05–0.35 partial pressure range.

The surface morphology and elemental composition of the samples were studied using a scanning electron microscope (SEM, Hitachi, S-3000N) combined with an energy dispersive X-ray (EDX) attachment. The accelerating voltage was 5.0 kV.

Powder X-ray diffraction (XRD) measurements of the catalysts were carried out on a computerized PANalytical X'Pert Pro diffractometer with Cu Kα (λ = 0.15406 nm) radiation. The data of 2θ from 20 to 80° were collected at 8°/min with the step size of 0.07°.

Visible Raman spectra of the catalysts were collected at room temperature on a Spex 1877 D triplemate spectrograph with spectral resolution of 2 cm^{-1}. A 532 nm DPSS diode-pump solid semiconductor laser was used as the excitation source and the power output was about 40 mW. Before measurements, the samples were well ground and mounted into a spinning holder to avoid thermal damage during scanning. The Raman signals were collected with conventional 90° geometry and the time for recording each spectrum was about 1000 ms. All Raman spectra used in this paper were original and unsmoothed.

The XPS of CeO$_2$, TiO$_2$ and CeO$_2$-TiO$_2$ were recorded on a scanning X-ray microprobe (PHI Quantera, ULVAC-PHI, Inc.) using Al Kα radiation (1486.7 eV). Binding energies of Ce 3d and O 1s were calibrated using C 1s peak (BE = 284.8 eV) as standard.

3. Results and discussion

3.1. NH$_3$-SCR activity of CeO$_2$-TiO$_2$ catalyst

The NH$_3$-SCR activities of CeO$_2$-TiO$_2$, CeO$_2$, and TiO$_2$ under a fixed GHSV of 250,000 h^{-1} are shown in Fig. 1. The pristine CeO$_2$ showed rather poor SCR activity in the whole temperature range with a maximum NO$_x$ conversion of 26%, while pristine TiO$_2$ did not exhibit any SCR activity at temperatures below 425 °C. However,
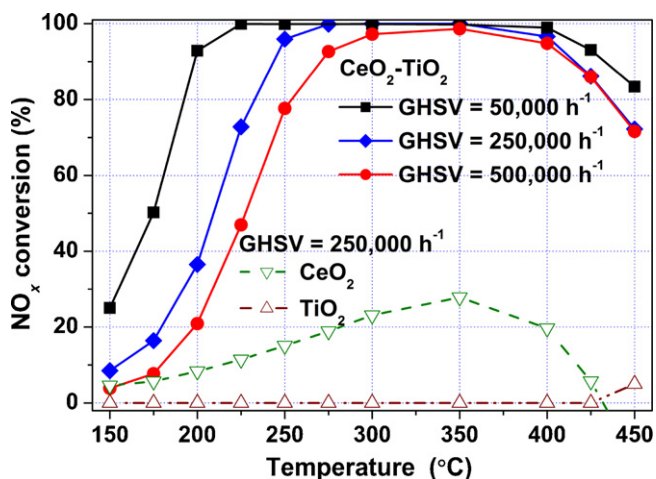
Fig. 1. NH$_3$-SCR activity of CeO$_2$-TiO$_2$ catalyst under different GHSV (50,000, 250,000 and 500,000 h^{-1}) and CeO$_2$ and TiO$_2$ under GHSV of 250,000 h^{-1}. Reaction conditions: [NO] = [NH$_3$] = 500 ppm, [O$_2$] = 5 vol.%, and N$_2$ balance.

the CeO$_2$-TiO$_2$ catalyst presented excellent NH$_3$-SCR activity in a broad temperature range. This result indicates that a synergistic effect for the NH$_3$-SCR reaction might exist between Ce species and Ti species.

The NH$_3$-SCR catalyst usually undergoes different GHSV in different working conditions of the diesel vehicles, thus the influence of GHSV on NO$_x$ conversion over the CeO$_2$-TiO$_2$ catalyst was also investigated (Fig. 1). The CeO$_2$-TiO$_2$ catalyst showed over 90% NO$_x$ conversion in a wide temperature range from 200 to 425 °C under a GHSV of 50,000 h^{-1}. With increasing GHSV, the low temperature SCR activity of the catalyst decreased somewhat. However, it still exhibited an excellent performance under a GHSV of 250,000 h^{-1} and even showed high resistance to a GHSV of 500,000 h^{-1}, which is important for its practical use on diesel vehicles to reduce the volume of the SCR catalytic converter.

3.2. Comparison with V$_2$O$_5$-WO$_3$/TiO$_2$ and Fe-ZSM-5 catalysts and the influence of high temperature calcination

V$_2$O$_5$-WO$_3$/TiO$_2$ and Fe-ZSM-5 are two types of NH$_3$-SCR catalysts which have been industrially and commercially used for NO$_x$ abatement from diesel exhaust. To better evaluate the NH$_3$-SCR performance of the CeO$_2$-TiO$_2$ catalyst, comparative SCR activity tests over V$_2$O$_5$-WO$_3$/TiO$_2$ and Fe-ZSM-5 catalysts were also carried out (Fig. 2). The NO$_x$ conversion over the CeO$_2$-TiO$_2$ catalyst was almost the same as that over V$_2$O$_5$-WO$_3$/TiO$_2$ (Fig. 2A), while the N$_2$ selectivity over the CeO$_2$-TiO$_2$ catalyst was much higher than that over V$_2$O$_5$-WO$_3$/TiO$_2$ in the high temperature range (Fig. 2B). Compared with the Fe-ZSM-5 catalyst, the operation temperature window of the CeO$_2$-TiO$_2$ catalyst was more than 50 °C lower under the same GHSV, with similar N$_2$ selectivity above 95% in the whole temperature range. The high NH$_3$-SCR activity and N$_2$ selectivity over a broad temperature range are important characteristics of the CeO$_2$-TiO$_2$ catalyst in regards to its practical utilization.

To evaluate the thermal stability of the catalyst, the influence of high temperature calcination on CeO$_2$-TiO$_2$ and V$_2$O$_5$-WO$_3$/TiO$_2$ was investigated (Fig. 2A). After high temperature calcination at 800 °C, the V$_2$O$_5$-WO$_3$/TiO$_2$-800 lost almost all the NH$_3$-SCR activity in the whole temperature range. However, the low temperature activity of the CeO$_2$-TiO$_2$-800 catalyst was still obviously higher than that of Fe-ZSM-5, indicating its high resistance to thermal shock. In short, the CeO$_2$-TiO$_2$ catalyst is a potential candidate for the catalytic removal of NO$_x$ from mobile sources, especially diesel engines with wide exhaust temperature ranges and high GHSV.
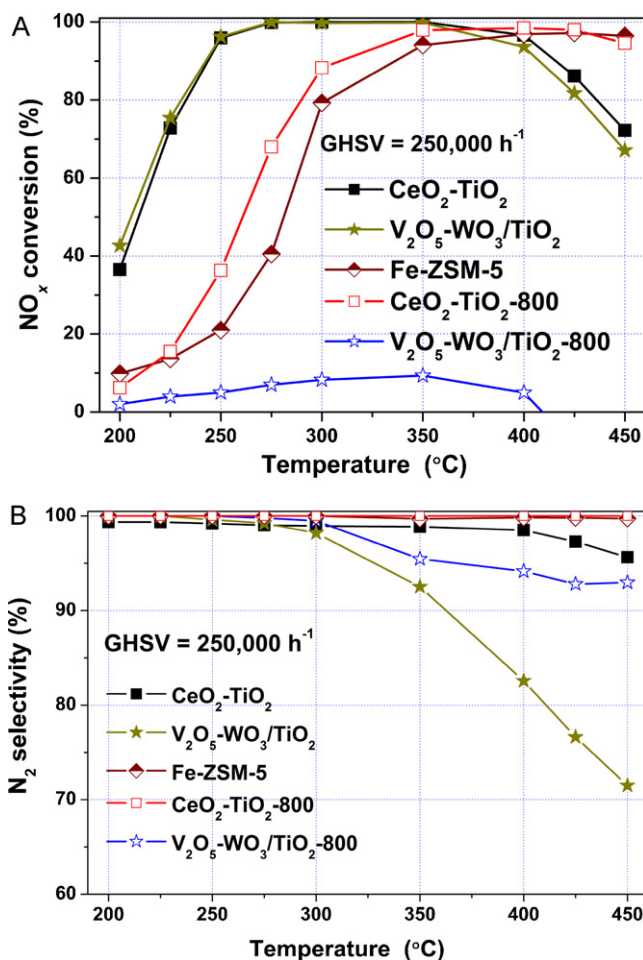

Fig. 2. Comparison of (A) NH$_3$-SCR activity and (B) N$_2$ selectivity of CeO$_2$-TiO$_2$ catalyst (calcined at 500 and 800 °C) with those of V$_2$O$_5$-WO$_3$/TiO$_2$ and Fe-ZSM-5 catalysts. Reaction conditions: [NO] = [NH$_3$] = 500 ppm, [O$_2$] = 5 vol.%, N$_2$ balance and GHSV = 250,000 h^{-1}.

3.3. NH$_3$-SCR activity of CeO$_2$-TiO$_2$ monolith catalyst

To evaluate the CeO$_2$-TiO$_2$ catalyst under more realistic conditions, a monolith catalyst with 130 g/L loading was prepared and tested under the same SCR condition as granulated catalysts and in the presence of H$_2$O, CO$_2$ and C$_3$H$_6$ (Fig. 3). Although the monolith catalyst was tested under a lower GHSV (20,000 h^{-1}), the ratio of sample weight to gas flow (W/F) of the tested monolith catalyst (0.023 g s/cm^3) was actually much lower than that of the tested granulated catalyst under the GHSV of 50,000 h^{-1} (0.054 g s/cm^3). Thus, it is not surprising that the NO$_x$ conversion over the monolith catalyst under GHSV of 20,000 h^{-1} was lower than that over granulated catalyst under GHSV of 50,000 h^{-1} in the low temperature range.

In the presence of 5% H$_2$O, 5% CO$_2$ and 250 ppm C$_3$H$_6$, the low temperature NO$_x$ conversion over the monolith catalyst decreased, while the high temperature NO$_x$ conversion increased, which was mainly associated with the influence of H$_2$O (the blocking of active sites in the low temperature range and the inhibition of unselective oxidation of NH$_3$ in the high temperature range). The monolith catalyst exhibited over 90% NO$_x$ conversion from 250 to 450 °C under a GHSV of 20,000 h^{-1} in the presence of H$_2$O, CO$_2$, and C$_3$H$_6$, indicating that it is a promising catalyst for NO$_x$ abatement from diesel engine exhaust. Further investigations on the H$_2$O and SO$_2$ effects and thermal stability of the CeO$_2$-TiO$_2$ catalyst are currently being conducted.

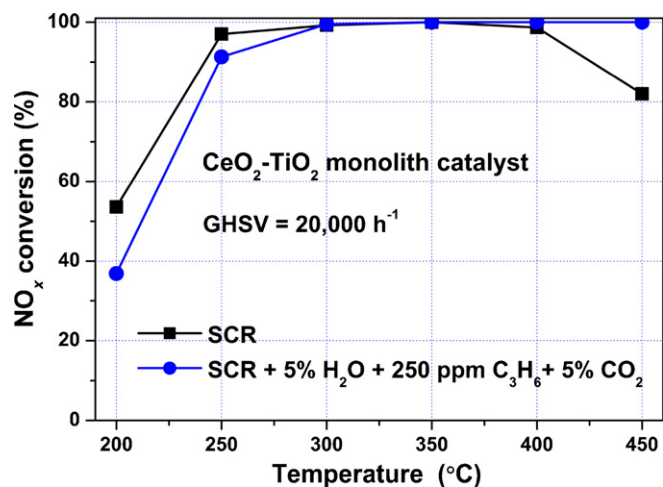**Fig. 3.** NH$_3$-SCR activity of CeO$_2$-TiO$_2$ monolith catalyst. Reaction conditions: [NO] = [NH$_3$] = 500 ppm, [O$_2$] = 5 vol.%, [H$_2$O] = 5 vol.% (when used), [CO$_2$] = 5 vol.% (when used), [C$_3$H$_6$] = 500 ppm (when used), N$_2$ balance and GHSV = 20,000 h^{-1}.
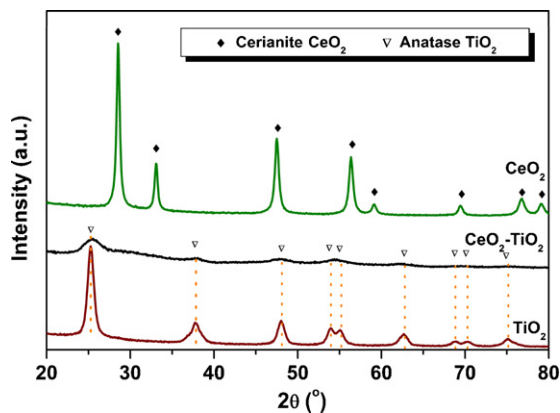

Fig. 4. XRD patterns of CeO$_2$-TiO$_2$, CeO$_2$ and TiO$_2$.

3.4. XRD results and Raman spectra

Fig. 4 shows the XRD patterns of the CeO$_2$, TiO$_2$, and CeO$_2$-TiO$_2$ catalysts. No crystalline phase ascribed to Ce species was observed in CeO$_2$-TiO$_2$, suggesting that Ce existed as highly dispersed species. The average crystallite sizes of TiO$_2$ were calculated by Scherrer's equation and are shown in Table 1. With the introduction of Ce, the average crystallite size of TiO$_2$ decreased from 11.1 to 7.6 nm, indicating that the Ce species inhibited the growth of anatase TiO$_2$ crystallite, which also resulted in the higher BET surface area of CeO$_2$-TiO$_2$ catalyst than that of pristine TiO$_2$ (Table 1).

Fig. 5 shows the visible Raman spectra of the CeO$_2$, TiO$_2$, and CeO$_2$-TiO$_2$ catalysts. The pristine CeO$_2$ and TiO$_2$ samples showed typical Raman shifts attributed to CeO$_2$ (F_{2g} mode at 465 cm^{-1}) [28,29] and TiO$_2$ (B_{1g} mode at 400 cm^{-1}, A_{1g} mode at 521 cm^{-1} and E_g mode at 648 cm^{-1}) [29,30], respectively. When the Ce species co-existed with the Ti species in the CeO$_2$-TiO$_2$ catalyst, no peak assigned to CeO$_2$ was detected, and the typical peaks of TiO$_2$ in

Table 1
BET surface area and average TiO$_2$ crystallite size (calculated by Scherrer equation from XRD results) of the samples.

Sample	BET surface area (m^2/g)	TiO$_2$ Crystallite size (nm)
CeO$_2$	46.1	–
CeO$_2$-TiO$_2$	125.7	7.6
TiO$_2$	106.7	11.1

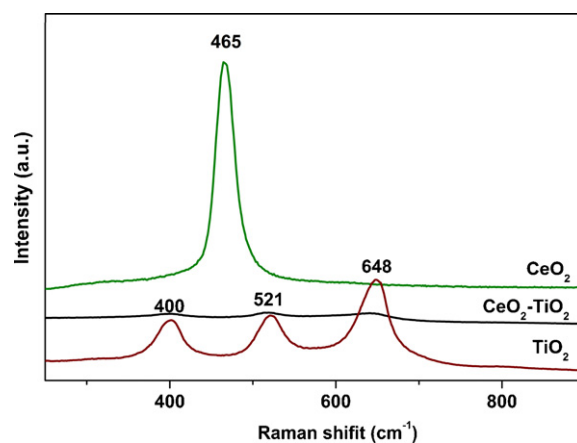**Fig. 5.** Raman spectra of CeO$_2$-TiO$_2$, CeO$_2$ and TiO$_2$ (λ_{ex} = 532 nm).
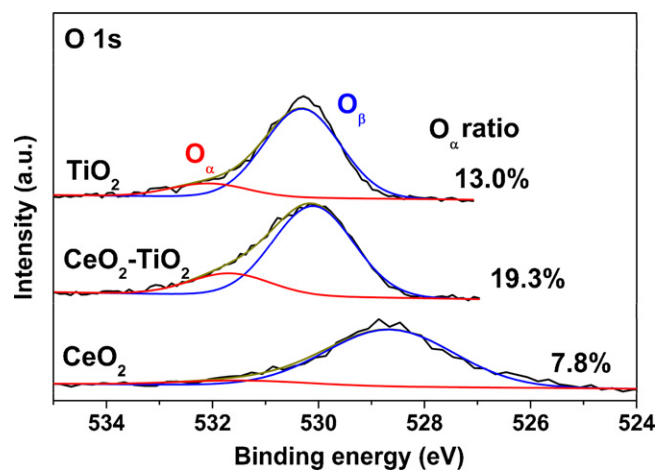

Fig. 6. XPS results of O 1s on CeO$_2$, TiO$_2$ and CeO$_2$-TiO$_2$.

CeO$_2$-TiO$_2$ were much weaker than those in pristine TiO$_2$, which is in good agreement with the XRD results in Fig. 4. It was reported that nano-crystalline CeO$_2$ is the main active phase over Ce-Ti based catalyst [25,26], thus the highly dispersed CeO$_2$ on TiO$_2$ by the coexistence of Ce and Ti species could increase the amount of active sites on the surface of CeO$_2$-TiO$_2$.
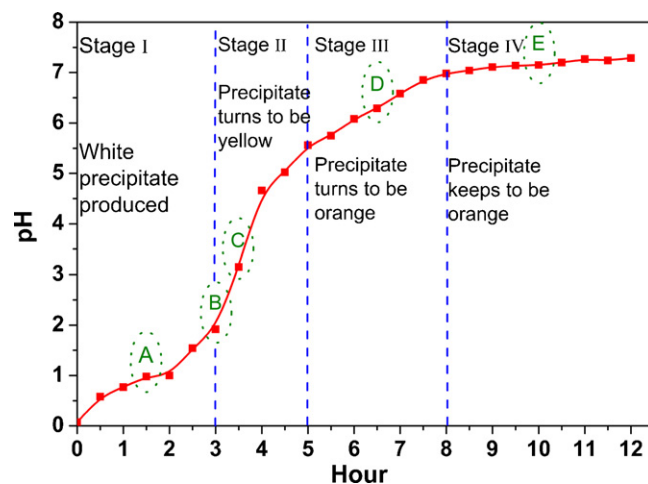

Fig. 7. The pH variation of the mixed solution during the preparation of the CeO$_2$-TiO$_2$ catalyst by the optimized homogeneous precipitation method.
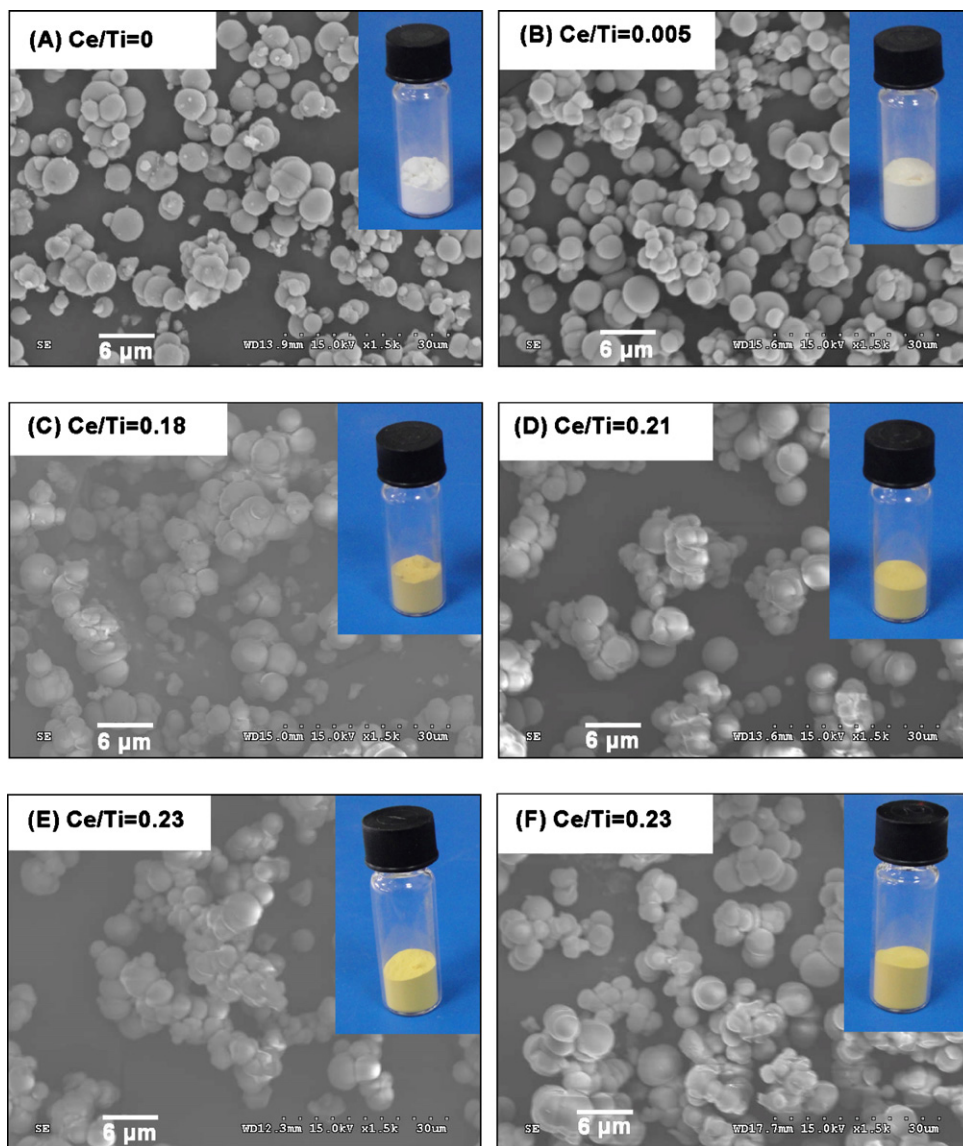
Fig. 8. SEM images and Ce/Ti molar ratios (determined by EDX analysis) of the samples prepared with different precipitation time. (A) 1.5 h; (B) 3 h; (C) 3.5 h; (D) 6.5 h; (E) 10 h and (F) 12 h.

3.5. XPS results of O 1s

The XPS results of O 1s on pristine CeO_2, TiO_2 and CeO_2-TiO_2 catalysts are shown in Fig. 6. The O 1s peak was fitted into two sub-bands by searching for the optimum combination of Gaussian bands with correlation coefficients (r^2) above 0.99. The sub-bands at lower binding energy corresponded to the lattice oxygen O^{2-} (denoted as O_β), and the sub-bands at higher binding energy corresponded to the surface adsorbed oxygen (denoted as O_α), such as O_2^{2-} or O^- belonging to defect-oxide or hydroxyl-like group [27]. The O_α ratio on CeO_2-TiO_2 (19.3%) calculated by $O_\alpha/(O_\alpha + O_\beta)$ was much higher than those on pristine CeO_2 (7.8%) and TiO_2 (13.0%), which means that the synergistic effect between Ce and Ti species resulted in more surface oxygen vacancies. Usually, O_α is more reactive than O_β in oxidation reactions due to its higher mobility [22]. Therefore, the higher O_α ratio on CeO_2-TiO_2 was beneficial for the NO oxidation to NO_2 in the SCR reaction, and thereby facilitated the "fast SCR" reaction and enhanced the $deNO_x$ efficiency at low temperatures.

3.6. Formation process of the CeO_2-TiO_2 catalyst

The above results demonstrate that homogeneous precipitation produced highly dispersed CeO_2 on TiO_2 and the prepared CeO_2-TiO_2 catalyst was highly active in the NH_3-SCR reaction. Thus, we determined the formation process of the CeO_2-TiO_2 catalyst during preparation.

Fig. 7 shows that the pH of the mixed solution increased with preparation time during the homogeneous precipitation process. The initial pH of the mixed $Ce(NO_3)_3 \cdot 6H_2O$, $Ti(SO_4)_2$, and urea solution was nearly zero due to the strong acidity of $Ti(SO_4)_2$. With urea hydrolyzation, the pH of the solution increased quickly in the first hour, after which a white precipitate was gradually produced and the increase in pH slowed down. After 3 h of heating, the pH of the solution showed a sharp increase and the precipitate turned yellow. The pH then steadily increased to about 7.0 and the precipitate gradually turned orange. After 8 h of heating, there was no significant change in the pH of the mixed solution or color of the precipitate.

Fig. 8 shows the SEM images of the samples at 10k magnification prepared under different precipitation times, as well as the Ce/Ti molar ratios of the samples determined by EDX. All samples consisted of spherical particles with diameters varying from 1 to 5 μm. The particle size of these samples observed with SEM was much larger than the average crystallite sizes of TiO_2 calculated by XRD (Table 1, 7.6 nm for CeO_2-TiO_2 and 11.1 nm for pristine TiO_2), indicating that each spherical particle was not a single crystallite but an agglomerate of many single crystallites. According to the EDX results, the Ce/Ti molar ratios in the samples prepared with the precipitation time of (A) 1.5 h, (B) 3 h, (C) 3.5 h, (D) 6.5 h, (E) 10 h and (F) 12 h were 0, 0.005, 0.18, 0.21, 0.23 and 0.23, respectively, indicating a gradually increase in the Ce/Ti molar ratio with precipitation time.

Based on the above results, the formation process of the CeO_2-TiO_2 catalyst was proposed. The Ti species was firstly precipitated when the pH of the mixed solution was between 1.0 and 2.0, and then the Ce species was precipitated uniformly onto the precipitated Ti species following the rapidly increase in pH to above 2.0. Accompanied with the increase in the Ce/Ti molar ratio during the precipitation process, the size of the precipitated spherical particles also increased. The process of homogenous precipitation is very important for the production of highly dispersed CeO_2 on TiO_2, which is probably a main reason for its excellent activity and high resistance to GHSV under SCR conditions.

4. Conclusions

The CeO_2-TiO_2 catalyst was prepared by an optimized homogeneous precipitation method for NH_3-SCR of NO_x in the presence of excess oxygen. The catalyst showed excellent NH_3-SCR activity and N_2 selectivity in a wide temperature range and exhibited good catalytic performance, even under a rather high GHSV of 500,000 h^{-1}. The CeO_2-TiO_2 catalyst showed much better N_2 selectivity than V_2O_5-WO_3/TiO_2 and presented much higher low temperature SCR activity than Fe-ZSM-5, even after high temperature calcination at 800 °C. The monolith catalyst of CeO_2-TiO_2 showed high NO_x conversion in a wide temperature range, even in the presence of H_2O, CO_2, and C_3H_6, which indicated that CeO_2-TiO_2 is a promising catalyst for NO_x abatement in diesel engine exhaust.

The process of homogenous precipitation is crucial for the production of highly dispersed active CeO_2 on TiO_2, which is very important for the high SCR activity of CeO_2-TiO_2 catalyst. The synergistic effects between CeO_2 and TiO_2 in the CeO_2-TiO_2 catalyst can inhibit the growth of anatase TiO_2 crystallite, which results in higher BET surface area. In addition, the synergistic effects between CeO_2 and TiO_2 can induce higher O_α ratio on the CeO_2-TiO_2 catalyst, which is beneficial for the high SCR activity of the catalyst at low temperatures.

References

[1] P. Granger, V.I. Parvulescu, Chem. Rev. 111 (2011) 3155–3207.
[2] T.V. Johnson, Int. J. Engine Res. 10 (2009) 275–285.
[3] Z. Liu, S.I. Woo, Catal. Rev. 48 (2006) 43–89.
[4] G. Busca, L. Lietti, G. Ramis, F. Berti, Appl. Catal. B 18 (1998) 1–36.
[5] S. Roy, M.S. Hegde, G. Madras, Appl. Energy 86 (2009) 2283–2297.
[6] S. Brandenberger, O. Kröcher, A. Tissler, R. Althoff, Catal. Rev. 50 (2008) 492–531.
[7] R.Q. Long, R.T. Yang, J. Am. Chem. Soc. 121 (1999) 5595–5596.
[8] A. Ma, W. Grünert, Chem. Commun. (1999) 71–72.
[9] G. Carja, G. Delahay, C. Signorile, B. Coq, Chem. Commun. (2004) 1404–1405.
[10] L. Xu, R.W. McCabe, R.H. Hammerle, Appl. Catal. B 39 (2002) 51–63.
[11] L. Li, J. Chen, S. Zhang, F. Zhang, N. Guan, T. Wang, S. Liu, Environ. Sci. Technol. 39 (2005) 2841–2847.
[12] J.H. Park, H.J. Park, J.H. Baik, I.S. Nam, C.H. Shin, J.H. Lee, B.K. Cho, S.H. Oh, J. Catal. 240 (2006) 47–57.
[13] J.H. Kwak, R.G. Tonkyn, D.H. Kim, J. Szanyi, C.H.F. Peden, J. Catal. 275 (2010) 187.
[14] D.W. Fickel, E. D'Addio, J.A. Lauterbach, R.F. Lobo, Appl. Catal. B 102 (2011) 441.
[15] L. Ren, L. Zhu, C. Yang, Y. Chen, Q. Sun, H. Zhang, C. Li, F. Nawaz, X. Meng, F. Xiao, Chem. Commun. 47 (2011) 9789.
[16] F. Liu, H. He, C. Zhang, Chem. Commun. (2008) 2043–2045.
[17] F. Liu, K. Asakura, H. He, Y. Liu, W. Shan, X. Shi, C. Zhang, Catal. Today 164 (2011) 520–527.
[18] F. Liu, H. He, C. Zhang, Z. Feng, L. Zheng, Y. Xie, T. Hu, Appl. Catal. B 96 (2010) 408–420.
[19] Z. Si, D. Weng, X. Wu, J. Li, G. Li, J. Catal. 271 (2010) 43–51.
[20] Y. Li, H. Cheng, D. Li, Y. Qin, Y. Xie, S. Wang, Chem. Commun. (2008) 1470–1472.
[21] L. Chen, J. Li, M. Ge, J. Phys. Chem. C 113 (2009) 21177–21184.
[22] Z. Wu, R. Jin, Y. Liu, H. Wang, Catal. Commun. 9 (2008) 2217–2220.
[23] K. Krishna, G.B.F. Seijger, C.M. Bleek, H.P.A. Calis, Chem. Commun. (2002) 2030–2031.
[24] T. Gu, Y. Liu, X. Weng, H. Wang, Z. Wu, Catal. Commun. 12 (2010) 310–313.
[25] W. Xu, Y. Yu, C. Zhang, H. He, Catal. Commun. 9 (2008) 1453–1457.
[26] W. Shan, F. Liu, H. He, X. Shi, C. Zhang, ChemCatChem 3 (2011) 1286–1289.
[27] F. Liu, H. He, Y. Ding, C. Zhang, Appl. Catal. B 93 (2009) 194–204.
[28] J. Twu, C.J. Chuang, K.I. Chang, C.H. Yang, K.H. Chen, Appl. Catal. B 12 (1997) 309–324.
[29] J. Fang, X. Bi, D. Si, Z. Jiang, W. Huang, Appl. Surf. Sci. 253 (2007) 8952–8961.
[30] K. Nagaveni, M.S. Hegde, G. Madras, J. Phys. Chem. B 108 (2004) 20204–20212.